2014 IEEE International Conference on Robotics & Automation (ICRA)
Hong Kong Convention and Exhibition Center
May 31 - June 7, 2014. Hong Kong, China

# Autonomous Dynamic Driving Control of Wheeled Mobile Robots

Jaemin Yoon, Jong-Hyun Oh, Joo-Hyun Park, Suhwan Kim, Dongjun Lee

***Abstract*— We propose a novel control framework to enable nonholonomic wheeled mobile robots (WMRs) to autonomously drive in an environment with the speed fast enough so that the dynamics effect (e.g., Coriolis effect) is not negligible, yet, still less than a certain threshold to prevent slippage at the wheels. For this, instead of the Newtonian vehicle modeling, we adopt Lagrange-D'Alembert formulation, which then allows us to explicitly relate the system's state/control with the constraint force, so that we can predict/detect possibility of a given motion's violating the no-slip condition. We present a scheme to generate a no-slip/collision-free timed-trajectory for the WMRs using this Lagrange-D'Alembert formulation. We also propose a backstepping-based control law, which enables the WMR to track the generated trajectory while respecting its nonholonomic constraints. Experiment, using a modified commercial radio-controlled car, is performed to verify the theory.**

## I. Introduction

Wheeled mobile robots (WMRs) have been extensively studied, yet, majority of their autonomous control results are focused on their kinematics control, assuming that their driving speed is slow enough so that the dynamics effect are negligible and/or the nonholonomic constraints (i.e., no-slip condition) are somehow enforced all the time (e.g., [1], [2], [3], [4], [5], [6], [7], [8], [9]). Our ultimate goal is to extend the current capability of the autonomous control for the nonholonomic WMRs toward their **dynamic** driving with fast driving speed.

This we believe would be possible given the substantially-enhanced sensors, actuators and computing systems, as evidenced by the recent progress of autonomous control to achieve aggressive and even acrobatic behavior of quadrocopters [10], [11]. Many hobbyists can perform such dynamic driving of the WMR. However, to our knowledge, such dynamic driving considering slip has very rarely achieved through autonomous control, and, in this paper, we provide a first step toward this autonomous control of dynamic driving of WMRs.

More specifically, as a first step toward this dynamic autonomous driving of WMRs, in this paper, we consider the problem where a WMRs (i.e., radio-controlled car: see Fig. 1) is required to drive with a speed as fast as possible while preventing slippage in an environment filled with some obstacles. Dynamic driving of utilizing slippage rather than preventing it will be studied in a future publication. The key challenge to achieve this dynamic, yet, still no-slip, driving is then how to ensure the driving speed be as fast as possible, yet, only to the extent the (static) friction can provide enough constraint force to maintain no-slip condition of the wheels.

Research supported in part by the Basic Science Research Program (2012-R1A2A2A0-1015797) of the National Research Foundation (NRF) of Korea funded by the Ministry of Education, Science & Technology (MEST) and Advanced Automotive Research Center (AARC) at SNU. J. Yoon and D. J. Lee are with the Department of Mechanical & Aerospace Engineering and IAMD, Seoul National University, Seoul, 151-744, Republic of Korea. J-H. Oh, J-H. Park and S. Kim are with the Department of Electrical & Computer Engineering, Seoul National University, Seoul, 151-744, Republic of Korea. Corresponding author: Dongjun Lee (djlee@snu.ac.kr).

Fig. 1. Autonomously-controlled radio-controlled car (Traxxas Slash©: http://traxxas.com).

To analyze this interplay between the (nonholonomic) WMR's dynamic effect and the friction, there are two ways of modeling the WMRs: 1) Lagrange-D'Alembert equation [12], [13], which typically assumes no-slip condition for each wheel, thus, more suitable when the speed of the vehicle is slow so that the friction can provide necessary traction to prevent slippage; and 2) Newtonian dynamics equation with "magic" formula [14], [15], which has been widely utilized for analyzing vehicle dynamics, is more suitable to address fast driving with slippage, yet, typically requires to solve all the dynamics equations to obtain any quantity of interests.

In this paper, in contrast to other works on dynamic driving with possible slippage, we rely on the Lagrange-D'Alembert formulation to model the WMRs. More precisely, we first generate collision-free path for the WMR in the environment with obstacles as a combination of arcs and straight lines similar to the case of optimal motion generation of Dubins car [16]. Then, for each path segment and their concatenation, we produce a timed-trajectory, that guarantees no-slip condition be enforced through the driving. For this, we utilize Lagrange-D'Alembert formulation to explicitly relate the vehicle's motion and the necessary friction to prevent the wheel slippage, that is,

$$\lambda = (A(q)M^{-1}(q)A^T(q))^{-1}[A(q)M^{-1}(q)\tau + \dot{A}(q)\dot{q}] \quad (1)$$

where $\lambda \in \Re^m$ is the Lagrange multiplier, $A(q)$ is the matrix characterizing the nonholonomic no-slip constraint, $M(q)$ is the inertia matrix, $\tau$ is the torque input, and $q \in \Re^n$ is the configuration of the WMR. Then, for each timed-trajectory segment, we can explicitly compute the constraint force to prevent slippage. If we generate WMR's motion so that this constraint force is less than the maximum (static) friction force on each segment and at their concatenations, we can then enforce no-slip condition throughout the whole dynamic driving. For this, we can exploit the well-known time-scaling

property of the Lagrange-D'Alembert equation [17], [18]. We also derive a backstepping feedback control law to drive the nonholonomic/dynamic WMR to track this no-slip timed-trajectory, and validate the proposed control framework via simulation as well as via experiment using hacked radio-controlled car (Fig. 1).

We believe the Lagrange-D'Alembert formulation has the following advantages over the Newtonian formulation for the modeling of dynamic driving with possible slippage, although the latter has been *de facto* modeling tool thereof: it allows us to explicitly compute necessary friction force to predict whether a wheel will slip or even trigger that; and its robot-like dynamics structure allows us to apply the well-known time-scaling property of, and control design techniques developed for, the standard robotic systems.

Some relevant results to this paper are as follow. The results in [9], [19], [20] are based on the purely-kinematic model, thus, limited to slow-driving and not suitable for dynamic driving. On the other hand, the schemes proposed in [3], [21], [22] assume the no-slip condition be somehow enforced all the time, excluding any possibility of slip, which may occur by the control action itself. The problem of robotic vehicle drifting control has been recently studied in [23], [24], [25], which utilize Newtonian modeling, thus, not exploring potential benefits of the Lagrange-D'Alembert formulation as stated above. This paper is an extension of our prior results in utilizing the Lagrange-D'Alembert dynamics and passivity property of mechanical systems with nonholonomic constraints [26], [27].

The rest of the paper is organized as follows. Lagrange-D'Alembert dynamics formulation of WMR is presented in Sec. II. Path planning and trajectory generation guaranteeing no-slip condition are proposed in Sec. III. Backstepping-based trajectory control law, which takes into account the nonholonomic constraint of the WMR, is then presented with simulation results in Sec. IV. Experimental results with some details on our own radio-controlled driving vehicle are provided in Sec. V. Concluding remarks are then given in Sec. VI.

## II. Lagrange-D'Alembert Dynamics of WMR Bicycle Model

To derive the dynamics of the radio-controlled car WMR in Fig. 1, we simplify its dynamics as that of the bicycle as frequently done in vehicle dynamics/control community to approximate full-dynamics of the vehicle and design a simplified control for that. This bicycle model for our WMR is depicted in Fig. 2, where $(x, y, \theta, \delta)$ are the WMR's mass center position, yaw angle, and steering angle of the front wheel; and $d_1, d_2 > 0$ are the distances of the rear and front wheels from $(x, y)$.

We define the configuration of the bicycle WMR s.t.,

$$q := [x, y, \theta, \alpha, \beta, \delta]^T \in \Re^6$$

where $\alpha, \beta$ are the rotation angles of the front and rear wheels. The no-slip condition of the two wheels can then be written by

$$A(q)\dot{q} = 0 \tag{2}$$

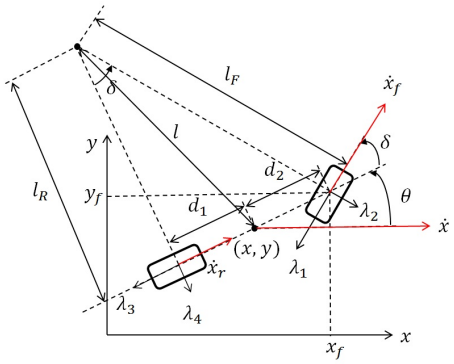


Fig. 2. Bicycle model of radio-controlled WMR with instantaneous center of rotation.

with

$$A(q) := \begin{bmatrix} \mathrm{c}_{\delta+\theta} & \mathrm{s}_{\delta+\theta} & d_2\,\mathrm{s}\,\delta & -r & 0 & 0 \\ -\mathrm{s}_{\delta+\theta} & \mathrm{c}_{\delta+\theta} & d_2\,\mathrm{c}\,\delta & 0 & 0 & 0 \\ \mathrm{c}\,\theta & \mathrm{s}\,\theta & 0 & 0 & -r & 0 \\ -\mathrm{s}\,\theta & \mathrm{c}\,\theta & -d_1 & 0 & 0 & 0 \end{bmatrix} \in \Re^{4\times 6}$$

where $\mathrm{c}\,\theta = \cos\theta$, $\mathrm{s}\,\theta = \sin\theta$, $\mathrm{c}_{\delta+\theta} = \cos(\delta+\theta)$, $\mathrm{s}_{\delta+\theta} = \sin(\delta+\theta)$, and $r > 0$ is the radius of the wheels. Note that the first two lines of (2) are no-slip conditions of the front wheel for the longitudinal and lateral directions, whereas the last two lines that of the rear wheel. This constraint (2) is in so called Pfaffian form and constitutes nonholonomic constraints [12].

Since a potential energy is absent in the bicycle WMR in Fig. 2, the Lagrangian $\mathcal{L}$ is simply given by its kinetic energy, i.e., $\mathcal{L}(q, \dot{q}) = \kappa(\dot{q}) := (1/2)\dot{q}^T M \dot{q}$, where the inertia matrix $M \in \Re^{6\times 6}$ is also given by a constant matrix s.t.,

$$M = \begin{bmatrix} m & 0 & 0 & 0 & 0 & 0 \\ 0 & m & 0 & 0 & 0 & 0 \\ 0 & 0 & I+J & 0 & 0 & J \\ 0 & 0 & 0 & I_F & 0 & 0 \\ 0 & 0 & 0 & 0 & I_R & 0 \\ 0 & 0 & J & 0 & 0 & J \end{bmatrix}$$

where $m, I, I_F, I_R, J > 0$ are respectively the mass and the moment of inertia of the vehicle, the moment of inertia of the two wheels and that of the front wheel along the steering direction. Then, the Lagrange-D'Alembert equation of the bicycle WMR dynamics is given by

$$M\ddot{q} + A^T(q)\lambda = \tau \tag{3}$$

where $A^T(q)\lambda$ is the constraint force, with the Lagrange multiplier $\lambda =: (\lambda_1, \lambda_2, \lambda_3, \lambda_4) \in \Re^4$ characterizing its magnitude; and

$$\tau = [0, 0, 0, \tau_F, \tau_R, \tau_\delta]^T \in \Re^6$$

with $\tau_F, \tau_R$ being the torque input for the rolling motion of the front and rear wheels, and $\tau_\delta$ for the steering motion of the front wheel. Here, note that we do not have a direct control for the translation and rotation of the vehicle body.

Our radio-controlled WMR in Fig. 1 is four-wheeled drive with differentials at the front, rear axles and center. Even so, similar to its wide applications in vehicle dynamics, we think

the bicycle model in Fig. 2 would be a reasonable simplification suitable for the control design of this paper. And our radio-controlled WMR splits the motor torque evenly between the front and rear with center open differential, i.e., $\tau_F = \tau_R = 0.5\tau_M$, where $\tau_M$ is motor torque. Other details on our radio-controlled WMR will be presented in Sec. V.

We can then see from (2) that $(\lambda_1, \lambda_2)$ and $(\lambda_3, \lambda_4)$ in (3) respectively represent the magnitude of the longitudinal and lateral constraint forces at the front and rear wheels to enforce each wheel's no-slip condition. This then means that, the front wheel (or rear wheel, resp.) will not slip if

$$\sqrt{\lambda_1^2 + \lambda_2^2} \leq \mu_s F_{Fz} \quad (\text{or } \sqrt{\lambda_3^2 + \lambda_4^2} \leq \mu_s F_{Rz}, \text{ resp.}) \quad (4)$$

where $F_{Fz}, F_{Rz}$ are the normal reaction force at the front and rear wheels exerted by the ground, which are given by

$$F_{Fz} \approx \frac{d_1}{d_1 + d_2} mg, \quad F_{RZ} \approx \frac{d_2}{d_1 + d_2} mg \quad (5)$$

from $F_{Fz} + F_{Rz} = mg$ and $d_1 F_{Rz} - d_2 F_{Fz} + h(\lambda_1 \cos\delta - \lambda_2 \sin\delta + \lambda_3) = 0$, with the assumption that $h \approx 0$ (i.e., with no weight-transfer between the front and rear wheels). Of course, it is also possible to include the effect of weight transfer while considering non-zero $h$. In this case, $F_{Fz}, F_{Rz}$ can still be computed as a function of $q, \dot{q}, \tau$, as $\lambda_i$ can be obtained from (1) as a function thereof. And $\mu_s$ is the known static friction coefficient. Some papers (e.g. [28], [29]) suppose method that can estimate the friction coefficient in real time in order to know friction coefficient precisely, but in this paper, we spare it for a future publication.

From (3), we can then obtain the "reduced" dynamics along the velocity directions respecting the constraints (2). That is, from the nonholonomic constraints (2), we can write

$$\dot{q} = \mathcal{D}(q)\eta \quad (6)$$

where the columns of $\mathcal{D}(q) \in \Re^{6\times 2}$ constitute the null space $A(q)$ (i.e., $A(q)D(q) = 0$) and $\eta := [\eta_1, \eta_2]^T \in \Re^2$. In particularly, if we choose

$$D(q) = \begin{bmatrix} \frac{r}{d_1+d_2}[d_1 \,\mathrm{c}_{\delta+\theta} + d_2 \,\mathrm{c}\,\delta\,\mathrm{c}\,\theta] & 0 \\ \frac{r}{d_1+d_2}[d_1 \,\mathrm{s}_{\delta+\theta} + d_2 \,\mathrm{c}\,\delta\,\mathrm{s}\,\theta] & 0 \\ \frac{r}{d_1+d_2}\,\mathrm{s}\,\delta & 0 \\ 1 & 0 \\ \mathrm{c}\,\delta & 0 \\ 0 & 1 \end{bmatrix} \in \Re^{6\times 2}$$

then, $\eta_1 = \dot{\alpha}, \eta_2 = \dot{\delta}$ respectively represents the linear velocity of the WMR vehicle body and the front wheel steering angular rate.

By applying (6) to (3), the "reduced" dynamics equation is achieved s.t.,

$$H(q)\dot{\eta} + Q(q,\dot{q})\eta = \mathcal{D}^T\tau \quad (7)$$

where $H(q) := \mathcal{D}^T(q)M\mathcal{D}(q) \in \Re^{2\times 2}$ is symmetric and positive-definite reduced inertia matrix and $Q(q,\dot{q}) := \mathcal{D}^T(q)M\dot{\mathcal{D}}(q) \in \Re^{2\times 2}$ with $\dot{H} - 2Q$ being skew-symmetric. Reduced Dynamics equation (7) shows that the first low describes the forward dynamics on a segment, and second low determine instantaneous curvature under the no-slip condition.

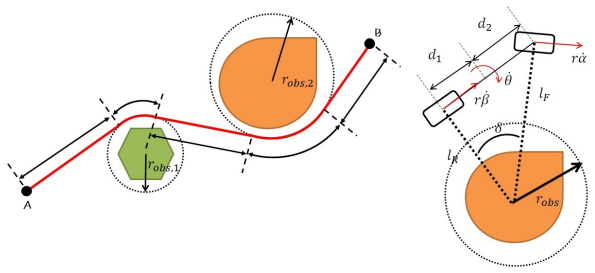


Fig. 3. Generated path consisting of arc and straight line segments.

One of the key advantage of using Lagrange-D'Alembert formulation (3) as compared to the Newtonian modeling is then that, given the vehicle motion (i.e., $q(t), \dot{q}(t)$) and control input $\tau$, we can *explicitly* compute from (1) these constraint forces $\lambda_i$ and use it to see if this motion $(q(t), \dot{q}(t))$ would be feasible under the no-slip condition. This advantage will be used to generate no-slip trajectory generation in the next Sec. III.

## III. Path Generation and Trajectory Generation for Dynamic Driving

In this paper, what we want here is to control the WMR to autonomously drive in the obstacle-cluttered environment with the speed as fast as possible, yet, only to the extent permissible by the friction to enforce no-slip condition as specified by (4). For this, similar to the optimal path generation for Dubins car [16], we first produce the collision-free path as composed of straight line segments and arc segments, each with a constant curvature. See Fig. 3.

If the no-slip conditions are preserved both for the front and rear wheels, as shown in Fig. 3, their velocity should be all along the longitudinal direction with zero component along the lateral direction. We can also define the instantaneous center of rotation, which, in this case, should be on the line perpendicular to the rear wheel center. Let us denote by $l_R$ and $l_F$ the instantaneous curvature at the rear and front wheels. We then have, from Fig. 3,

$$l_F = \frac{d_1 + d_2}{\sin\delta}, \quad l_R = l_F \cos\delta = \frac{d_1 + d_2}{\tan\delta} \quad (8)$$

that is, the instantaneous curvatures are completely determined by the steering angle $\delta$ under the no-slip condition.

Also, from $l_F\dot{\theta} = r\dot{\alpha}$ and $l_R\dot{\theta} = r\dot{\beta}$, we have

$$\dot{\theta} = \frac{r}{d_1 + d_2}\dot{\alpha}\sin\delta, \quad \dot{\beta} = \dot{\alpha}\cos\delta \quad (9)$$

that is, if the no-slip condition is enforced, vehicle's linear motion can be completely specified either by $\dot{\alpha}$ or $\dot{\beta}$, while its angular rate $\dot{\theta}$ by this linear velocity and the steering angle $\delta$. This suggests that, if we choose $l_R > r_{\text{obs}}$, the WMR will not collide with the obstacles. See Fig. 3. Note again that this curvature condition in fact determines the desired steering angle $\delta$ from (8).

Once this collision-free path is constructed as a composition of straight line and arc segments, we then generate timed-trajectory on them. Here, the goal is to generate the trajectory with fastest speed permissible by the no-slip condition. For this, as stated above, we utilize the relation

(1) to explicitly relate the given trajectory and the constraint force required to produce that motion while enforcing no-slip condition.

More precisely, given a candidate trajectory $(q(t), \dot{q}(t), \ddot{q}(t))$ on a segment, we can compute the required constraint force $\lambda$ from (1) with $\tau$ also computed from (7). We can then check the possibility of violation of the no-slip condition via (4).

We now present a procedure for the trajectory generation for the straight line segment and the arc segment:

- **Straight line segment:** For this, $\delta = 0$ and we can also assume $\theta = c$ with $c \in \Re$ being a constant, from the symmetry of the WMR's dynamics w.r.t. $\theta$ and $\dot{\theta} = 0$. On the straight line segment, we also design a timed-trajectory $\alpha(t)$, which then completely describes the motion of the vehicle on the segment.
  Given this $\alpha(t)$ with $\dot{\delta} = \ddot{\delta} = 0$, we can further compute the required motor torque $\tau_M$ by using (7) and $\tau_F = \tau_R = 0.5\tau_M$, i.e.,
  $$(mr^2 + I_F + I_R)\ddot{\alpha}(t) = \tau_M, \quad \tau_\delta = 0$$
  Moreover, we can write the relation (1) s.t.,
  $$\begin{aligned}\lambda &= (AM^{-1}A^T)^{-1}[AM^{-1}\tau + \dot{A}(q)\dot{q}] \\ &= [-\frac{mr^2 - I_F + I_R}{2r}\ddot{\alpha}, 0, -\frac{mr^2 + I_F - I_R}{2r}\ddot{\alpha}, 0]^T\end{aligned}$$
  This then implies that the required constraint force $\lambda$ is purely proportional to $\ddot{\alpha}(t)$, thus, we can prevent the wheel slippage at the front and rear wheels by adjusting $\ddot{\alpha}(t)$ so as to comply with the no-slip condition (4), i.e., $|\ddot{\alpha}| \leq \frac{\mu_s g}{r}$ with $d_1 = d_2, I_F = I_R$. The above equations about $\tau$ and $\lambda$ also mean that, if the trajectory $\alpha(t)$ is time-scaled by a constant factor $s_t > 0$ (i.e., new time $t = s_t t'$), the torque $\tau_M$ should be scaled by $s_t^2$ and so is the constraint force $\lambda$ as well. It is very useful property for motion planning with no slip condition enforced.
- **Constant curvature arc segment:** Since the curvature of the arc is solely determined by $\delta$ (see Fig. 3), we have $\dot{\delta} = 0$, although, in this case, $\dot{\theta} \neq 0$. On the arc segment, let us define timed-trajectory $\alpha(t)$. Then, similar to above, this $\alpha(t)$ completely describes the vehicle motion on the segment with its yaw rate $\dot{\theta}$ also given by (9). Moreover, with $\dot{\delta} = 0$ and $\ddot{\delta} = 0$, we can also compute the required torque to produce this timed-trajectory by using (7) and $\tau_F = \tau_R = 0.5\tau_M$, i.e.,
  $$f_1(\delta)\ddot{\alpha}(t) = \tau_M, \quad f_2(\delta)\ddot{\alpha}(t) = \tau_\delta$$
  where $f_1(\delta), f_2(\delta)$ are some functions of $\delta$ only. We can then write the relation (1) s.t.,
  $$\begin{aligned}\lambda &= (AM^{-1}A^T)^{-1}[AM^{-1}\tau + \dot{A}(q)\dot{q}] \\ &= [k_1\ddot{\alpha}, k_{21}\ddot{\alpha} + k_{22}\dot{\alpha}^2, k_3\ddot{\alpha}, k_{41}\ddot{\alpha} + k_{42}\dot{\alpha}^2]^T\end{aligned}$$
  where $k_{21}, k_{22}, k_{41}, k_{42}$ are some functions of $\delta$ only, and $k_{21} > 0, k_{22}, k_{41}, k_{42} < 0$ for our radio-controlled WMR. Therefore, given $\alpha(t)$ and $\delta$, we can compute the constraint force $\lambda$ and check if the motion is feasible under the no-slip condition (4). In this case,
  $$\begin{cases}\dot{\alpha} \leq \sqrt{\frac{0.5\mu_s mg}{\max(|k_{22}|, |k_{42}|)}} & \text{if } \ddot{\alpha} = 0 \\ \dot{\alpha} < \sqrt{\frac{0.5\mu_s mg}{\max(|k_{22}|, |k_{42}|)}} & \text{if } \ddot{\alpha} \neq 0\end{cases}$$
  because $k_{21}$ and $k_{22}$ are not same sign, $k_{41}$ and $k_{42}$ are same sign, so, if $\ddot{\alpha} \neq 0$ and $\dot{\alpha} \geq \sqrt{\frac{0.5\mu_s mg}{\max(|k_{22}|, |k_{42}|)}}$ (maximum speed), $\lambda_2$ or $\lambda_4$ exceed static friction force and WMR slips. Therefore, WMR should drive constant speed in arc segment in order to drive with a speed as fast as possible while preventing slippage. The above equations about $\tau$ and $\lambda$ also manifests the well-known time-scaling property on the arc segment as well as, with the time-scaling factor $s_t > 0$, again, $\tau_M$ will be scaled by $s_t^2$ and so is the constraint force $\lambda$. As stated above, it is very useful property for motion planning with no slip condition enforced.

To sum up, if we want to drive as fast as possible while preventing slippage, in arc segment, WMR should drive with constant maximum speed. And, in straight line segment, WMR should drive with maximum acceleration, and then maximum deceleration until WMR's speed reaches maximum speed of arc segment (determined by $\delta$) just before entering arc segment. Since, if WMR decelerates just before entering the arc segment in order to reach maximum speed of arc segment enforced by no-slip condition, WMR satisfies no-slip condition while concatenating each segment, so WMR should not slip while concatenating straight line and arc segment. Also, in straight line segment, driving with maximum acceleration and deceleration is the fastest driving technique while preventing slippage. Similar to above, in arc segment, driving with maximum speed while preventing slippage is optimal (If WMR accelerate, it cannot drive faster than maximum speed).

## IV. Backstepping-Based Trajectory Tracking Control Design

To allow WMR to track the no-slip trajectory on each segment as defined above, we design a feedback trajectory tracking control. Since the WMR is under the nonholonomic constraint, we also utilize the backstepping technique [30] in designing our tracking control. For that, let us denote by $p_f^d(t) := (x_f^d(t), y_f^d(t))$ the desired trajectory of the front wheel when the vehicle follows the no-slip timed-trajectory on each segment. Since, on each segment, the motion of the vehicle is only one-dimensional, this $p_f^d(t)$ can completely specify the vehicle motion at each time. We then want

$$e := (x_f - x_f^d, y_f - y_f^d)^T \to 0$$

where $p_f := (x_f, y_f) := (x + d_2 \,\mathrm{c}\,\theta, y + d_2 \,\mathrm{s}\,\theta)$ is the position of the front wheel.

Then, if we can achieve $\dot{e} = -k_e e$, $k_e > 0$, we will have $e \to 0$ exponentially. However, this is not always possible, since, in general, we have

$$\begin{aligned}\dot{x}_f &= r\dot{\alpha}\cos(\theta + \delta) = \dot{x}_f^d - k_e(x_f - x_f^d) + \nu_x \\ \dot{y}_f &= r\dot{\alpha}\sin(\theta + \delta) = \dot{y}_f^d - k_e(y_f - y_f^d) + \nu_y \qquad (10)\end{aligned}$$

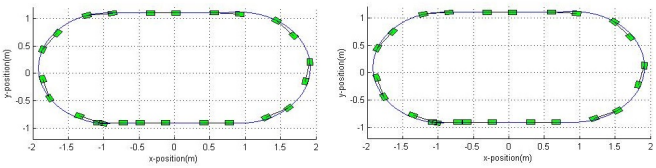


Fig. 4. Simulation of autonomous dynamic driving of bicycle-type WMR using Lagrange-D'Alembert formulation and Newtonian modeling.

where $\nu_x, \nu_y$ are the error, which occur since there is no guarantee that $\dot{\alpha}$ and $\theta + \delta$ are as such to satisfy the above equations with $\nu_x = \nu_y = 0$.

To deal with this mismatch, define $V_1 := \frac{1}{2} e^T e$. Then,

$$\dot{V}_1 = -k_e e^T e + e^T \nu$$

since $\dot{e} = -k_e e + \nu$ as shown above with $\nu := (\nu_x, \nu_y) \in \Re^2$. Let us augment $V_1$ s.t., $V := V_1 + \frac{1}{2\gamma} \nu^T \nu$. Then, we have

$$\dot{V} = -k_e e^T e + \frac{1}{\gamma} \nu^T (\dot{\nu} + \gamma e)$$

which suggests the following backstepping law

$$\dot{\nu} = -\gamma e - k_\nu \nu \tag{11}$$

to achieve

$$\dot{V} = -k_e e^T e - k_\nu \nu^T \nu$$

implying $(e, \nu) \to 0$ exponentially.

This backstepping law (11) then needs to be decoded into the real control inputs $\tau_M, \tau_\delta$. For this, following the idea of [30], by differentiating

$$\nu = \begin{pmatrix} r\dot{\alpha} \cos(\theta + \delta) - \dot{x}_f^d + k_e (x_f - x_f^d) \\ r\dot{\alpha} \sin(\theta + \delta) - \dot{y}_f^d + k_e (y_f - y_f^d) \end{pmatrix}$$

from (10) and plugging it into (11), we can obtain

$$\begin{bmatrix} r\,\mathrm{c}_{\theta+\delta} & -r\dot{\alpha}\,\mathrm{s}_{\theta+\delta} \\ r\,\mathrm{s}_{\theta+\delta} & r\dot{\alpha}\,\mathrm{c}_{\theta+\delta} \end{bmatrix} \begin{pmatrix} \ddot{\alpha}_d \\ \dot{\delta}_d \end{pmatrix} \tag{12}$$
$$= \ddot{p}_f^d + k_\nu \dot{p}_f^d - k_e \dot{e} - (\gamma + k_e k_\nu) e - r\dot{\alpha} \begin{pmatrix} k_\nu\,\mathrm{c}_{\theta+\delta} - \dot{\theta}\,\mathrm{s}_{\theta+\delta} \\ k_\nu\,\mathrm{c}_{\theta+\delta} + \dot{\theta}\,\mathrm{c}_{\theta+\delta} \end{pmatrix}$$

where $\ddot{\alpha}_d, \dot{\delta}_d$ are now the desired command for the front wheel and the steering angle. We can then design the control torques $\tau_M, \tau_\delta$ from (7), $\ddot{\delta} = -k_\delta(\dot{\delta} - \dot{\delta}_d)$ with $k_\delta > 0$ large enough and $\tau_F = \tau_R = 0.5\tau_M$. Then, we can show that, from the above exponential convergence, the error $(e, \nu)$ is ultimately bounded with the bound possible to made arbitrarily small by increasing the control gains $k_e, k_\nu, k_\delta$.

Simulation results of the proposed framework, including trajectory generation and tracking control, for the bicycle dynamics model, are presented in Fig. 4, where we can see that the bicycle WMR can drive among the obstacles with no slippage. The result on the left is using Lagrange-D'Alembert formulation and right result is using Newtonian modeling, which is almost same result on the left.

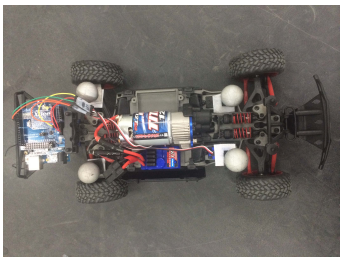

Fig. 5. Modified radio-controlled WMR.

## V. Experiments with Custom-Modified Radio-Controlled Car

Fig. 1 shows the top view of Traxxas Slash. The Slash is an electric powered, 2.4GHz radio controlled 1/16 scale 4WD car. It includes a receiver, an electronic speed control (ESC), steering servo, motor, and batteries. As the receiver grasps signals from the transmitter of a hand-held radio unit, the electronic speed control drives one Titan 550 motors by responding to the pulse width modulation (PWM) signal. The motors deliver on demand torque for wheels-up launches and maximum speed increases to over 30mph on one 6-cell NiMH battery packs.

Fig. 5 shows the top view of the developed autonomous vehicle. The receiver part of the Traxxas Slash are substituted with an Arduino to control steering stepper motors and Titan motors with PC. The Arduino is a single-board microcontroller to make using electronics in multidisciplinary projects more accessible. The length of a pulse sets the position of the stepper motor where they are used to provide actuation for steering the vehicle.

The developed vehicle is able to communicate with a PC base station. It is done through Xbee protocol. The protocol is intended for embedded applications requiring low data rates and low power consumption. One of the key features of Xbee is its wide range which can vary anywhere between 100 meters to 4 km. Also shown in Fig. 5 are markers to be used with VICON motion capture system to measure the position and orientation of the vehicle with 125Hz update rate. The sampling rate of the whole system is set to be 5ms with data sustained if their update rate is slower than 5ms.

For our radio-controlled WMR in Fig. 5, the control input is the motor torque $\tau_M$ and the steering angle $\delta$ not its torque $\tau_\delta$, since its steering is controlled by stepper motors. To address this, instead of $\tau_\delta$, we rather integrate $\dot{\delta}_d$ in (12) to construct $\delta_d$, i.e.,

$$\delta_d(t) = \delta_d(0) + \int_0^t \dot{\delta}_d(\tau) d\tau$$

and apply this $\delta_d(t)$ to the steering stepper motors. And WMR's mass m = 1.03kg, distances of the rear and front wheels from mass center position $d_1 = d_2 = 10.4cm$, and radius of wheels $r = 3.3cm$.

Experimental results with this modified radio-controller WMR are shown in Fig. 6, where the WMR is autonomously controlled to drive to track the timed-trajectory, which consists of line and arc segments and encloses an obstacle in

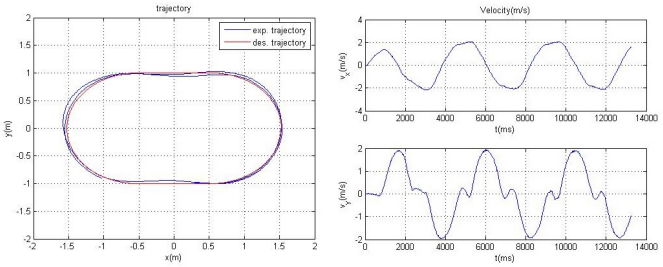


Fig. 6. Experimental results of trajectory tracking using modified radio-controlled WMR.

the center, with a speed close to the threshold of onset of slippage.

## VI. CONCLUSION

In this paper, we consider the autonomous control problem of dynamic driving of WMR with a fast speed yet with no slippage in an environment having some obstacles. For this, we utilize Lagrange-D'Alembert formulation, which, differently from the widely-used Newtonian vehicle model, allows us to directly relate the system's state and control to the required constraints force, thus, also to predict possibility of no-slip condition being violated. We also present a trajectory generation scheme to avoid collision with obstacles and slippage at the wheels. A backstepping-based control law is also presented to enable the bicycle-type WMRs to track the generated trajectory. Experiment with our custom-modified radio-controller high-speed vehicle is also performed to validate the framework.

Some possible future research topics include: 1) application of one-line tire friction coefficient estimation algorithm to real-time prediction of possibility of slippage; and 2) control synthesis to utilize the wheel slippage.

## REFERENCES


[1] C. Canudas de Wit and O. J. Sordalen. Exponential stabilization of mobile robots with nonholonomic constraints. *IEEE Transactions on Automatic Control*, 37(11):1791–1797, 1992.

[2] C. Samson. Time-varying feedback stabilization of car-like wheeled mobile robots. *International Journal of Robotics Research*, 12(1):55–64, 1993.

[3] I. Kolmanovsky and N. H. McClamroch. Developments in nonholonomic control problems. *IEEE Control Systems*, 15(6):20–36, 1995.

[4] J. P. Ostrowski. Computing reduced equations for robotic systems with constraints and symmetries. *IEEE Transactions on Robotics and Automation*, 15(1):111–123, 1999.

[5] P. Morin and C. Samson. Control of nonholonomic mobile robots based on the transverse function approach. *IEEE Transactions on Robotics*, 25(5):1058–1073, 2009.

[6] D. J. Lee. Passivity-based switching control for stabilization of wheeled mobile robots. In *In Proc. Robotics: Science & Systems*, pages 70–77, 2007.

[7] H. Yang and D. J. Lee. Cooperative grasping control of multiple mobile manipulators with obstacle avoidance. *In Proc. IEEE Int'l Conference on Robotics & Automation*, pages 828–833, 2013.

[8] K. D. Do, Z. P. Jiang, and J. Pan. Simultaneous tracking and stabilization of mobile robots: an adaptive approach. *IEEE Transactions on Automatic Control*, 49(7):1147–1151, 2004.

[9] M. Egerstedt, X. Hu, and A. Stotsky. Control of mobile platforms using a virtual vehicle approach. *IEEE Transactions on Automatic Control*, 46(11):1777–1782, 2001.

[10] O. Purwin and R. D'Andrea. Performing aggressive maneuvers using iterative learning control. *In Proc. IEEE Int'l Conference on Robotics & Automation*, pages 1731–1736, 2009.

[11] D. Mellinger, N. Michael, and V. Kumar. Trajectory generation and control for precise aggressive maneuvers with quadrotors. *In Proc. of Int'l Symposium on Experimental Robotics*, 2010.

[12] A. M. Bloch. *Nonholonomic mechanics and control*. Springer, New York, NY, 2003.

[13] R. M. Murray, Z. Li, and S. S. Sastry. *A mathematical introduction to robotic manipulation*. CRC, Boca Ranton, FL, 1993.

[14] R. Rajamani. *Vehicle dynamics and control*. Springer, New York, NY, 2006.

[15] E. Velenis, D. Katzourakis, E. Frazzoli, P. Tsiotras, and R. Happee. Steady-state drifting stabilization of rwd vehicles. *Control Engineering Practice*, 19(11):1363–1376, 2011.

[16] J. A. Reeds and L. A. Shepp. Optimal paths for a car that goes both forwards and backwards. *Pacific Journal of Mathematics*, 145(2):367–393, 1990.

[17] G. Sahar and J. M. Hollerbach. Planning of minimum-time trajectories for robot arms. *International Journal of Robotics Research*, 5(3):90–100, 1986.

[18] M. W. Spong, J. K. Holm, and D. J. Lee. Passivity-based control of bipedal locomotion. *IEEE Robotics & Automation Magazine*, pages 30–40, 2007.

[19] D. Wang and C. B. Low. Modeling and analysis of skidding and slipping in wheeled mobile robots: Control design perspective. *IEEE Transactions on Robotics*, 24(3):676–687, 2008.

[20] C. B. Low and D. Wang. Gps-based path following control for a car-like wheeled mobile robot with skidding and slipping. *IEEE Transactions on Control Systems Technology*, 16(2):340–347, 2008.

[21] J. Barraquand and J. C. Latombe. On nonholonomic mobile robots and optimal maneuvering. In *IEEE Int'l Symposium on Intelligent Control*, pages 340–347, 1989.

[22] R. M. Murray and S. S. Sastry. Nonholonomic motion planning: steering using sinusoids. *IEEE Transactions on Automatic Control*, 38(5):700–716, 1993.

[23] J. Yi, J. Li, J. Lu, and Z. Liu. On the stability and agility of aggressive vehicle maneuvers: a pendulum-turn maneuver example. *IEEE Transactions on Control Systems Technology*, 99(99):1–14, 2011.

[24] S. D. Cairano, H. E. Tseng, D. Bernardini, and A. Bemporad. Vehicle yaw stability control by coordinated active front steering and differential braking in the tire sideslip angles domain. *IEEE Transactions on Control Systems Technology*, 21(4):1236–1248, 2013.

[25] C. E. Beal and J. C. Gerdes. Model predictive control for vehicle stabilization at the limits of handling. *IEEE Transactions on Control Systems Technology*, 21(4):1258–1269, 2013.

[26] D. J. Lee. Passive decomposition and control of nonholonomic mechanical systems. *IEEE Transactions on Robotics*, 26(6):978–992, 2010.

[27] D. J. Lee. Passive configuration decomposition and practical stabilization of nonholonomic mechanical systems with symmetry. In *In Proc. IEEE Conference on Decision & Control*, pages 3620–3625, 2010.

[28] J. O. Hahn, R. Rajamani, and L. Alexander. Gps-based real-time identification of tire-road friction coefficient. *IEEE Transactions on Control Systems Technology*, 10(3):331–343, 2002.

[29] R. Rajamani, G. Phanomchoeng, D. Piyabongkarn, and J. Y. Lew. Algorithms for real-time estimation of individual wheel tire-road friction coefficients. *IEEE/ASME Transactions on Mechatronics*, 17(6):1183–1195, 2012.

[30] D. J. Lee. Distributed backstepping control of multiple thrust-propelled vehicles on a balanced graph. *Automatica*, 48(11):2971–2977, 2012.